Volcanic activity and magma plumbing system during caldera and post-caldera stage of Mashu volcano, eastern Hokkaido

*Keiji Wada[1], Yu Nakatsuka, Eiichi Sato[2], Yuya Okada[1]

1. Earth Science Laboratory, Hokkaido University of Education at Asahikawa, 2. Institute for Promotion of Higher Education, Kobe University

Mashu volcano, characterized by a caldera of 6 x 7 km diameter generated about 7500 years ago, is located at eastern ridge of Kutcharo caldera in the Akan-Shiretoko volcanic chain in eastern Hokkaido (Katsui et al., 1975). Mashu volcano started activities around 35 thousand years ago and has repeated explosive eruptions many times (Sumita, 1990; Hasegawa et al., 2009). Volcanic sequence of caldera stage and post-caldera stage during 14 thousand years has been well studied by Kishimoto et al. (2009) based on previous research of Katsui et al. (1975 and 1986). However, magma plumbing system during caldera stage and the following post-caldera stage, and stratigraphic relationship between post-caldera lavas and tephra deposits have not been cleared by petrological approach. We show plural magma chamber models at the caldera stage and eruptive sequence of post-caldera stage including four lavas. Major caldera formation of tephrostratigraphy of Ma-j, Ma-i, Ma-h, Ma-g, Ma-f (Kishimoto et al., 2009) was reviewed. According to the change of lithic fragments and existence of lithic-rich thin layers between pumice fall deposits, the location of the crater may have changed during the plinian eruptions. The most mafic compositions of bulk and minerals in Ma-g tephra has different compositional trend compared with other eruptive products of caldera-forming series. Ma-f large-volume pyroclastic flow deposit shows a wide compositional variations including the range of all other caldera-forming series products. These suggest existence of two different magma chambers of Ma-j, Ma-i, and Ma-h units and of Ma-g unit. It seems that both of the magma chamber eventually reached the catastrophic eruption of Ma-f unit. During the post-caldera stage (6000?-1000 years ago) magma activity was changed to the new plumbing system based on the bulk chemistry. Kamuishu-island lava dome (SiO_2=73.9wt.%) in the center of the caldera erupted at the beginning of a long dormant period after the caldera formation, after that Kamuinupuri small strato-cone was formed in the eastern edge of the caldera. The eruptive sequence of three lavas from Kamuinupuri was deduced by bulk and minerals chemistry. Kamuinupuri northwestern lava (SiO_2=68.5wt.%) erupted during the main activity of Kamuinupuri strato-cone formation (Ma-d tephra; SiO_2=63.9-69.4wt.%). After the Ma-d tephra activity Kamuinupuri western lava (SiO_2 =54.5-61.6wt.%) effused. The Kamuinupuri north lava (SiO_2=70.6wt.%) can be erupted after the Ma-c tephra layer eruption (2500-1500 years ago). At about 1000 years ago the latest explosive eruptions including plinian fall and pyroclastic flow (Ma-b tephra; SiO_2=67.0-69.3wt.%) occurred.

Keywords: Mashu volcano, caldera, magma plumbing system

Investigation on Funatsu Tainai lava tree molds in Kenmarubi-I lava flow

*Tsutomu Honda[1], Hiroshi Tachihara[1], Tadato Makita[1]

1. Vulcano-speleological Society

[Introduction]

Funatsu Tainai lava tree molds are a national natural monument located in the midstream area of Kenmarubi-I lava flow, and their measurement and investigation were carried out by K.Ogawa of Speleological Society and published as Yamanashi-ken natural monument urgent investigation report[1)]. The investigation is continued and new additional lava tree molds are found and named as Yamanashi-ken monument important material by NPO Vulcano-Speleological Society. The volcanologic knowledge obtained from the current state of those investigations will be reported.

[The lava flow thickness and yield strength]

Funatsu Tainai lava tree molds count many vertical lava tree molds among which main natural monument and monument important material are listed in Table.1. The depth of the vertical tree mold are between 2.1m and 5.4m. Most has 4 m-5 m of depth as shown in Table.2. A diameter of a tree in this area was at most 1.9 m. The depth of the vertical lava tree molds shows a lava flow thickness. H, and gradient angle α in this area is approximately 8 degree, so the Bingham yield strength:f_B can be estimated as f_B =6.9x104~1.9x105dyne/cm^2 from lava flow critical condition :$H=f_B/(\rho g \sin \alpha)$ of simple lava flow where ρ =2.5g/cm^3 and g=980cm/sec^3. This f_B is regarded as the proper value as basaltic lava of SiO_2 50.88wt% (Tsuya [4)]) or 51.1% (Takada [5)]), though it seems a little bit high because of the temperature fall at this area. This value agree with estimated value $5.0x10^4$~$1.5x10^5$dyne/cm^2 by Yamashita [6)]. Therefore Kenmarubi-I lava flow can be regarded as a simple lava flow defined by Walker [7,8)].

[Lava rib structure and surface tension estimated in Tainai]

Funatsu Tainai shows a complex lava tree molds which include lava stalactite from the ceiling and the ribbed wall formed by re-melting inside it[9)]. It's possible to estimate the surface tension of the lava from the pitch of the lava stalactite and ribbed wall[10)]. From instability onset conditions of melted liquid thin film, pitch(wave length) is shown as $P=2\pi(\gamma/g\rho)^{1/2}$,where γ is the surface tension of the lava and g is the gravity, and ρ is the density of the lava. Therefore it's possible to estimate a surface tension $\gamma = P^2 g \rho / 4\pi^2$ by measuring P of lava stalactite which hangs down from the ceiling inside the Tainai or from ribbed structure of side wall. The pitch obtained from Funatsu Tainai indicated in Fig.1 is P=3~4cm approximately, then, γ=560-990 dyne/cm is obtained as the surface tension. It's the reasonable value as surface tension of basaltic lava.

[Conclusion]

Similar results of yield strength and surface tension are also obtained for the Yoshida Tainai lava tree molds in the lava flow of Kenmarubi-II(SiO_2 51.2wt%[5)]). Kenmarubi-I and the Kenmarubi-II are regarded as a simple lava flow. These lava flows has so low thickness that could not make a lava tube cave. Without being buried, much of lava tree molds are left. So, the biggest complex lava tree mold in the world exists in this area[3)]. On the other hand, Aokigahara lava flow which has thick lava flow and high flow rate making a lot of lava tube caves indicates a compound lava flow. Further researches and investigations are under going for both Tainai lava tree molds.

References:

1) Yamanashi-ken natural monument urgent investigating committee and lava cave/tree mold are an investigation group of Ogawa:Yamanashi-ken natural monument urgent investigation report (1996), Yamanashi-ken Education Board , p182-344.

2) H.Tachihara,T.Makita (1998): 1997 1998 year lava tree mold report,NPO Vulcano-Speleological Society.
3) H.Tachihara (2011): Volcano cave and lava tree mold. Caving journal No.43,p15-17
4) H.Tsuya(1971): The geographical feature of Mt. Fuji and the geological feature. Mt. Fuji overall investigation report, Fuji Kyuko p71
5) A.Takada et al (2016): Fuji volcanic geologic map (2nd edition), National Institute of Advanced Industrial Science and Technology ,Geological Survey of Japan.
6) S.Yamashita et al (2002): Reproduction of the Kenmarubi Lava Flow by a Numerical Simulation :. Japan Geoscience Union Meeting V032-P022
7)G.P.L.Walker(1971):Compound and simple lava flows and flood basalts. Bull.Volcanol.35,p579-590
8) S.Umino (2007): Characteristics of Lava flows of Fuji volcano, Fuji Volcano, Yamanashi Institute of Environmental Sciences p269-283
9) T.Honda (1998): Physico-chemical Explanation for Remelting Process of Inner Surface Wall of Tainai Tree Molds Located on the Flank of Mt. Fuji. Journal of the Speleological Society of Japan,vol 23,p29-38
10) T.Honda (2015): Estimation of surface tension of lava from lava stalactite and lava stalagmite appeared in lava tube cave and tree mold. Japan Geoscience Union Meeting SVC46-07

Keywords: Lava tree mold, Kennmarubi-I lava flow, Funatsu tainai

Table.1 船津胎内縦樹型の深さと直径
（文献 1）から縦樹型のみを抽出したもの）

船津胎内縦樹型番号	深さ	直径
No, 1	3. 0m	1. 3m
No, 3	4. 9m	0. 6m
No. 4	4. 9m	0. 9m
No. 5	3. 0m	1. 3m
No. 6	4. 0m	1. 2m
No. 7	3. 6m	0. 9m
No. 8	3. 9m	1. 2m
No. 10	4. 3m	1. 5m
No. 12	4. 3m	0. 6m
No. 14	4. 9m	0. 6m
No. 18	5. 4m	1. 0m
No. 19	4. 8m	0. 8m
No. 21	4. 0m	1. 2m
No. 24	3. 0m	1. 3m
No. 25	5. 2m	0. 8m
No. 26	4. 6m	0. 6m
No. 29	3. 3m	1. 3x2. 7m
No. 38	2. 1m	0. 9m
No. 39	2. 3m	1. 6m
No. 40	2. 3m	0. 3m
No. 41	2. 9m	1. 6m
No. 42	4. 9m	1. 3m
記念物重要資料 No. 3	3. 9m	1. 1m
記念物重要資料 No. 105	2. 9m	1. 9m

Table.2 船津胎内縦樹型の深さと本数の分布

縦樹型の深さの範囲	樹型の本数
2. 0m-2. 9m	5
3. 0m-3. 9m	7
4. 0m-4. 9m	10
5. 0m-5. 4m	2

Fig.1 船津胎内の肋骨状溶岩とピッチの計測

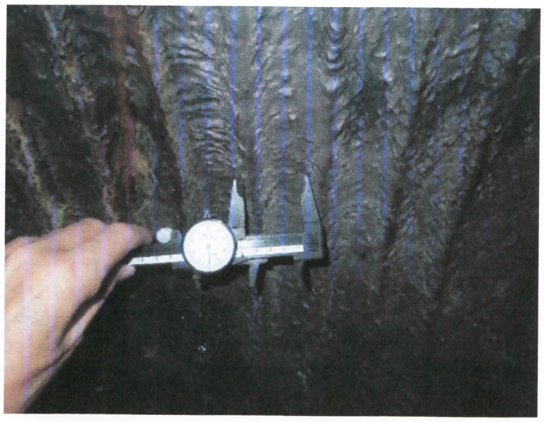

Frequency of volcanic eruptions and long-term magma discharge rate in sub-regions in Japan

*Koji Kiyosugi[1]

1. Organization of Advanced Science and Technology, Kobe University

Frequency of volcanic eruptions is an important factor to evaluate volcanic activity. Together with eruption magnitude, which is defined by mass of ejecta, frequency of eruptions can be used to estimate long-term magma discharge rate. Such estimation will provide an insight of material circulation through volcanoes. Calculating frequency of eruptions is, however, a challenging problem due to difficulty of estimating the amount of under-recording of volcanic eruptions. The main mechanisms of under-recording are absence of historical records, erosion and alteration of tephra deposits, burial of tephra deposits by younger deposits, disappearance of the source volcano itself due to burial or erosion, deposition of majority of tephra on the sea surface and occurrence of submarine eruption. In this study, I calculated frequency of volcanic eruptions and estimated long-term magma discharge rate in sub-regions in Japan, in which eruption records account for about 39 % of the entire set of eruptive events in the world.

I investigated the dataset of age and magnitude, M, of volcanic eruptions (M 2), which occurred in the Hokkaido, Tohoku, Izu, Central and Kyushu regions in Japan in recent about 2 million years. The analyzed data are compiled from documentation including Machida and Arai (2003), Committee for Catalog of Quaternary volcanoes in Japan (2000), Geological Survey of Japan, AIST (2014) and Hayakawa (2010). In estimating frequency of eruptions, under-recording of events was taken into account by modeling a decreasing trend of recording rate of analyzed volcanic eruptions with time.

The results of the analysis show that the frequency of eruptions (M 2) in those regions varies more than one order of magnitude. For relatively large eruptions (4 M 6), frequency of eruptions decays by a factor of about 10 for each successive eruption magnitude category. On the other hand, frequency of eruptions (2 M 4) decays by a factor of about 1.5 - 2.6, showing that the frequency of smaller eruptions is smaller than the frequency expected from the magnitude-frequency relationship of the relatively larger eruptions. One possible explanation of this small frequency is that smaller batch of magma is less buoyant and is more likely stuck in the crust.

The long-term magma discharge rate was calculated on the basis of the magnitude-frequency relationships in those regions. After considering the length of those subduction zones, the long-term magma discharge rate in Kyusyu, Central and Tohoku regions show similar value (2×10^{10} kg/ka/km). On the other hand, the long-term magma discharge rate in Hokkaido and Izu regions is about one third of that of the other regions. The smaller long-term magma discharge rate in the Hokkaido region than that in the Tohoku region is probably caused by an oblique subduction of the Pacific plate, which results in a smaller effective subduction velocity of the Pacific plate beneath the North American plate in the Hokkaido region than that in the Tohoku region. On the other hand, the similar amount of long-term magma discharge rates in different subduction zones, including the Tohoku, Central and Kyushu regions, suggest that such tectonic constraint is not significant. Furthermore, the estimated small magma discharge rate in the Izu region may be caused by insufficient estimation of the amount of under-recording of events. This region consists of small volcanic islands where wide-spread tephra deposits are less likely preserved, and hence eruptions in large eruption magnitude categories (M 6) are almost completely missing. In addition, no eruptions are recorded for some submarine volcanoes in this region. For these missing eruption categories and volcanoes, it is impossible to estimate the amount of under-recording of events. Therefore, additional statistical approach is required for more accurate estimation of frequency of eruption and long-term magma discharge rate in the region of oceanic islands.

Keywords: eruption database, frequency of eruption, long-term magma discharge rate

Formation process of the Omine pyroclastic cone in Niijima Island, Japan

*Reina NAKAOKA[1], Kazuhiko Kano[2], Keiko Suzuki-Kamata[1]

1. Kobe University, 2. Kagoshima University

On the Niijima Island, rhyolitic eruption started in 886 with generation of the Habushiura pyroclastic density current deposits followed by the growth of the Omine pyroclastic cone and the emplacement of the Mukaiyama lava. Sedimentary structures, emplacement temperatures and ash morphology indicate the Habushiura pyroclastic density current deposits were generated by shallow marine phreatomagmatic eruption (Nakaoka and Suzuki-Kamata, 2015). In this study, we discuss the eruption style and development of the Omine pyroclastic cone with sedimentary features of the deposits and paleomagnetism of the essential rock fragments.

The Habushiura pyroclastic density current deposits constitute a plateau rising over 100 m above sea level and the Omine pyroclastic cone rises 200 m above the plateau with a basal diameter of 2.7 km, without any indication of significant time break between the Omine pyroclastic cone such as weathered zone and structural disconformity. The summit is relatively flat being covered with the Mukaiyama lava but at least, five craters are confirmed in the eastern half.

The eruption products contain block-sized to lapilli-sized poorly to moderately vesicular fragments and blocky to platy ash particles of biotite rhyolite with minor accidental fragments. Juvenile fragments contain elongate vesicles but have a bulk density of 1.6–1.7 g/cm^3, larger than 0.8–1.3 g/cm^3 for the Habushiura pyroclastic density current. These clasts are accumulated in the cone commonly to form massive, poor sorted beds abundant in ash with a thickness of several 10 cm to 120 cm thick.

Upon thermal demagnetization, magnetization direction of the juvenile fragments becomes stable and parallel to the direction of the Earth's magnetic field of that time below 350-400 degree C. This implies that the juvenile fragments were emplaced below 350-400 degree C and magnetized while being cooled to the ambient temperature, consistent with that block-sized juvenile fragments have prismatic cracks and are occasionally disintegrated along the cracks.

These results collectively suggest that the Omine tuff cones are composed of the pyroclastic density current deposits produced by explosive interaction between the hot lava and external water or gravitational collapse of lava. The Habushiura pyroclastic density current deposits are also interpreted as the products of explosive interaction between the hot lava and external water but its emplacement temperature is below 300 degree C as estimated also by thermal demagnetization (Nakaoka and Suzuki-Kamata, 2015). This perhaps reflects lesser extent contribution of the ambient water to the eruption of Omine pyroclastic cone. Pyroclasts, however, could accumulate to build a pyroclastic cone but exceptionally where wet in direct contact with water vapor (Aranda-Gomez and Luhr, 1996; Kano and Takarada, 2007).

The effect of open water for flow and depositional mechanisms of Koya pyroclastic flow: an examination from the ignimbrites distributed on Tanega-shima

*Tomomi Yamane[1], Keiko Suzuki-Kamata[2]

1. Graduate School of Science, Kobe University, 2. Kobe Ocean-Bottom Exploration Center

Koya pyroclastic flow (Ui, 1973) is a large-scale pyroclastic flow occurred at the 7.3 ka (Fukusawa, 1995) Akahoya eruption of Kikai caldera. Akahoya eruption started from large-scale Plinian eruption which formed plinian pumice-fall deposit and intraplinian pyroclastic-flow deposit and terminated with eruption of Koya pyroclastic flow (Machida and Arai, 2003; Maeno and Taniguchi, 2007; Fujihara and Suzuki-Kamata, 2013). The Koya ignimbrite is distributed over the proximal islands (Iwo-jima and Take-shima) and the adjacent islands (Tanega-shima, Yaku-shima and Kuchinoerabu-jima) and the mainland of south Kyusyu (Satsuma and Osumi peninsulas) around Kikai caldera (Ui, 1973; Machida and Arai, 1978; Ono et al., 1982; Maeno and Taniguchi, 2007; Geshi, 2009; Fujihara and Suzuki-Kamata, 2013).

Although it is clear that Koya pyroclastic flow traveled across the sea because of the distribution of the ignimbrite and study of the Holocene relative sea-level change (e.g. Tanigawa et al., 2013), there is no discussion about the effect of open water for Koya pyroclastic flow.

Products of Akahoya eruption contain two types of volcanic glass shards. The one is "high-SiO_2 glass shards" (ca. 75 SiO_2 wt. %), and the other is "low-SiO_2 glass shards" (ca. 65 SiO_2 wt. %). The ratio of both types of glass shards shows vertical variation within the Koya ignimbrite (Fujihara and Suzuki-Kamata, 2013). Based on the ratio of both types of glass shards, Fijihara and Suziki-Kamata (2013) concluded that the early phase products of Koya pyroclastic-flow eruption contain only high-SiO_2 glass shards and low-SiO_2 magma started to erupt at later phase of the pyroclastic flow eruption.

To reveal the effect of open water, we adopted these methods, geological survey, chemical analysis of glass shards and thickness and pumice size measurement.

For chemical analysis of glass shards, matrix samples of the Koya ignimbrite on Tanega-shima in 4 sites were sampled from base to top with regular level interval. 40-100 glass shards were selected at each level and measured the major element composition by EPMA. While high-SiO_2 glass shards can be recognized throughout the ignimbrite, low-SiO_2 ones exist only at the upper level of it. The early phase products of Koya pyroclastic-flow eruption reached to Tanega-shima because this vertical variation is equal to that of the ignimbrites on proximal area, Satsuma peninsula and Osumi peninsula (Fujihara and Suzuki-Kamata, 2013). Lower contents of low-SiO_2 glass shards from upper most level compared with that of Osumi peninsula suggest that the flows which contain abundant in low-SiO_2 glass shards occured at the later phase of the pyroclastic flow eruption cannot reach to Tanega-shima. This is conformable the fact that the ignimbrites on Osumi peninsula are thicker than that of Tanega-shima.

The maximum pumice size (MPS) was measured from the Koya ignimbrites of Satsuma peninsula, Osumi peninsula and Tanega-shima. Proportional connection between MPS and distance over water (see Figure) suggests that Koya pyroclastic flow was experienced the successively selective loss of large pumice during traveling over water. From this proportional connection, the distal limit of Koya pyroclastic flow traveling over water estimated approximately 70 km from source (see Figure). Tanega-shima is located in almost the distal limit.

Based on above discussion, it is easy to estimate that Koya pyroclastic flow lost a great many amount of pyroclasts in the sea during traveling across the sea and the Koya ignimbrite widely lies on the sea floor

around Kikai caldera.

Keywords: Kikai caldera, Koya pyroclastic flow, the effect of open water, volcanic glass shards, Tanega-shima, distal limit of pyroclastic flow

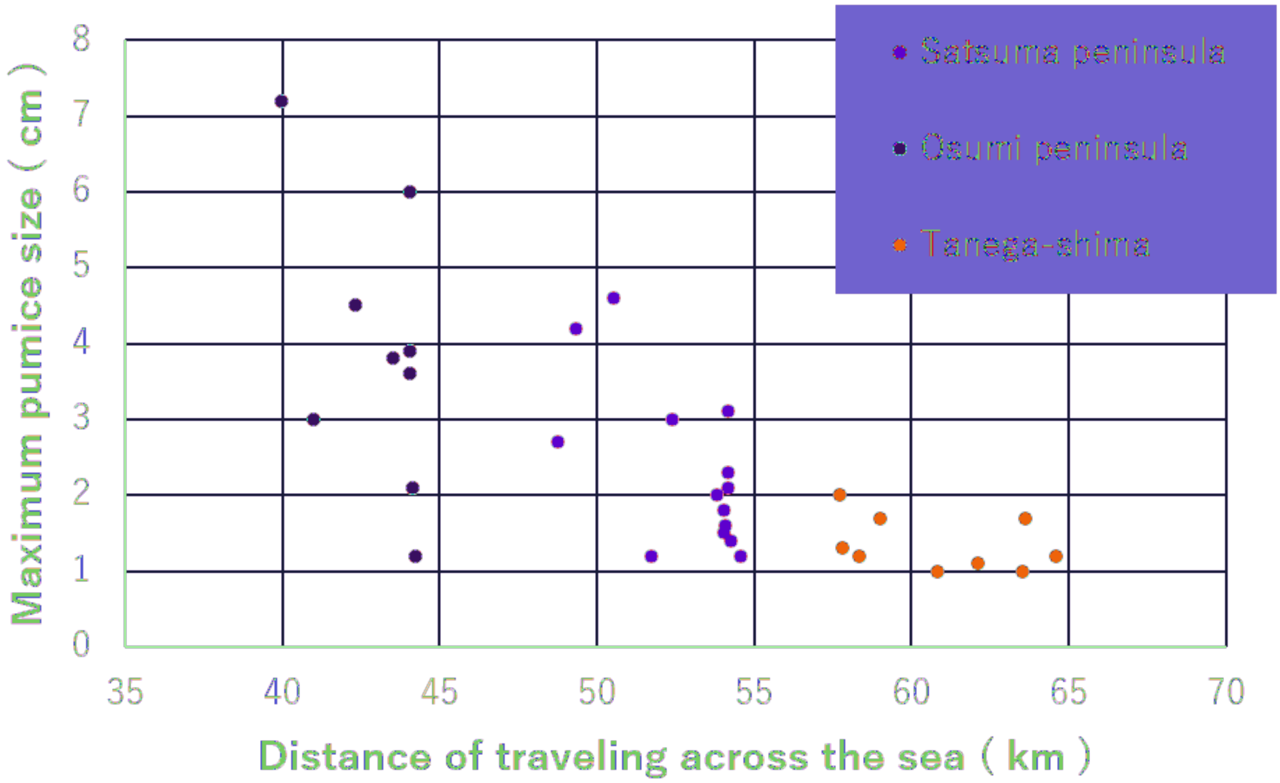

The distribution of Ikezuki tuff (Onikobe-Ikezuki tephra) in Shinjo and Mukaimachi basin, NE Japan

*Tsuyoshi Miyamoto[1], Yoshimi Hiroi[2], Masayoshi Fujino[3]

1. Center for Northeast Asian Studies, Tohoku University, 2. Graduated school of Science, Tohoku University, 3. HIGASHI NIPPON BROADCASTING CO,Ltd.

Within Shinjo basin in Yamagata prefecture, some of pyroclastic flow deposits are intercalated in gravel layer of Quaternary Systems. Especially the oldest and thickest pumice tuff (Torigoe tephra) in upper Yamaya formation is corresponded to Ikezuki tuff (Onikobe-Ikezuki tephra: O-Ik) distributing in Naruko-Onikobe area at the eastern side of the Ou Backbone range in Miyagi prefecture. From an eruption age of O-Ik, pyroclastic flow deposits and upper Yamaya formation in this basin are thought to be younger than 0.3 ka. Matu’ ura (2003) devided pyroclastic flow deposits over Torigoe tephra (O-Ik) into four tephra layers (Sakekawa, Izumikawa, Emakawa and Ushikuguri in ascending order). Large-scale pyroclastic eruption is only from both Naruko and Onikobe caldera since 0.3 ka around Shinjo basin. Though three large-scale pyorclastic flow deposits (Shimoyamasato, Nisaka, Yanagisawa tuff in ascending order) are observed after O-Ik within Naruko-Onikobe area, there is a possibility that only Shimoyamasato tuff distributes in Shinjo basin because Ushikuguri tephra, which is the youngest pyroclast, is covered with Dokusawa tephra (0.1 Ka). However four pyroclastic flow deposits are not correlated with Shimoyamasato tuff in previous studies, and the source of their flow deposits are unknown. Thus to clarify the source caldera of pyroclasts in Shinjo basin, we studied the pyroclastic flow deposits within both Shinjo and Mukaimachi basin based on the field survey and petrological studies (volcanic glass and mineral compositions analysis, bulk chemistry of essential pumice fragments). In consequence we report that Torigoe tephra is not O-Ik and all pyroclasts in upper Yamaya formation are older deposits than O-Ik tephra. In this study to avoid confusion, we use “Shinjo tuff” as a newly name, not Torigoe tephra.
From the field survey pyroclastic flow stratigraphy was identified to be nearly similar to one of Matsu’ ura(2003) except for one flow unit. Shinjo tuff, is the oldest and resemble to O-Ik, thickly distributes in all area of Shinjo basin. Although Emakawa tephra has as a same distribution as Shinjo tuff, the thickness decreases from north to south. No pyroclastic deposits are corresponding to Simoyamasato tuff as same as previous studies. Within Mukaimachi basin we could observe that Shimoyamasato tuff overlay the O-Ik. Though Gravel layer under O-Ik intercalates one pyoroclastic density current, five pyroclastic flow deposits within Shinjo basin are not present.
Shinjo tuff has similar features to O-Ik in field occurrence. Additionally volcanic glass compositions and heavy mineral assemblages using for tephra identification are nearly same between two pyroclasts, and Shinjo tuff was assumed to be same deposit as O-ik. But this study has determined to be two distinct pyroclasts from the difference of below three features.
1. Stratigraphy: though both O-Ik within Naruko-Onikobe area and Shinjo tuff was assumed directly to cover with the same volcanic ash layer, it was found that their ash layers are another deposits because they have distinct glass chemical composition. In addition O-Ik within Mukaimachi basin is covered by Simoyamasato tuff, while Shinjo tuff within Shinjo basin is overlain by other tuff.
2. Modal composition of heavy minerals: the contents of heavy mineral in Shinjo tuff are significantly lower than one of O-Ik.
3. Bulk chemical compositions of essential pumice fragments: despite of the effect of alternation two pyroclasts are distinguished in major element compositions, and are clearly divided in trace element composition, especially HFSE and Y which is not affected by the alternation.
O-Ik exists within Mukaimachi basin, not within Shinjo basin in the western side from source caldera. This

distribution implies that the flow path of O-Ik was limited by the western wall of Mukaimachi caldera. No distribution within Mukaimachi basin of five pyoroclastic flow deposits observed in Shinjo basin indicates that all pyrocalasts in upper Yamaya formation was older than O-Ik, this is very important to construct the evolution of Shinjo basin. Moreover it is possible from this insight that tuff in Yamaya formation were erupted from other caldera, not Naruko and Onikobe caldera. Especially the thickness changes of Emakawa tephra and Shinjo tuff might suggest that former tuff was derived from Sanzugawa caldera located on northern part of Shinjo basin, and later tuff was from Mukaimachi caldera.

Keywords: Ikezuki tuff, Shinjo tuff, Mukaimachi caldera

The source of Kamafusayama pyroclastic deposits and debris avalanche deposit, southern Fukushima prefecture, Japan

*Daisuke Sekine[1], Takeshi Hasegawa[1]

1. Ibaraki University Major in Science Department of Earth Science

1. Introduction
Kamafusayama pyroclastic deposits (KfPD, 0.59-0.41Ma)[2)3)4)] consist of dacitic to andesitic pyroclastic fall and flow deposits, distributed in the southern Fukushima. The main part of KfPD compose Kamafusayama (1510m.a.s.l). The KfPD has intermediate characteristics with respect to: 1) age, 2) distribution and 3) compositions between early Pleistocene felsic large-scale pyroclastic flow deposits (Shirakawa pyroclastic flow group, about1.51Ma-0.92Ma)[1)2)5)6)] and basaltic to andesitic Nasu stratovolcanic group (0.54Ma[7)] -present). Although clarifying the eruption history and magma processes of KfPD is essential for understanding the volcanism and magmatism in this area, detailed stratigraphy and source area have not been clearly revealed. We have carried out geological and petrological study of KfPD to reveal the stratigraphy and magmatic processes, and current results can be summarized as follows; 1) KfPD is divided into two eruption stages (Eruption stage 1 and 2) separated by a paleosol layer, 2) A debris avalanche (KfDa) deposit was found at the top of Eruption stage 1, 3) Compositional trends of Stage 1 and 2 are slightly different each other on K2O-SiO2 diagram, and 4) magma mixing was a common process in each stage.
In order to determine the source of KfPD, we investigated distributions and lateral change of thicknesses of the deposits. In addition, we compared the petrologic features (petrography and whole-rock chemistry) with adjacent volcanic rocks; Ksv (Kashi volcanic rocks (after 1.47~1.21Ma)[1)6)]) which is the older products of Kashiasahidake Volcano, Kav (Kashiasahidake Volcano(0.54Ma)[7)]) forming present edifice of Kashiasahidake Volcano, and Oshiromoriyama Lavas intruding in Ksv(Early Pleistocene)[1)]. In addition, petrologic characteristics of lava fragments in KfDa were also determined.
2. Field occurrences
Both of Eruption stage 1 and 2 of KfPD consist of alternative units of pyroclastic flow and fall deposits (Eruption stage 1 and 2 are composed of 7 and 13 units, respectively). There is no paleosol layer within the units in one stage. The thickness of KfPD air-fall units increase towards Kashiasahidake Volcano. KfDa is composed of tuffaceous matrix facies and block facies. The former contains white pumice, gray pumice, scoria, and lithic fragments of tuff and lava. The latter is materials incorporated from underlying layers and mega blocks (max 3.0m in diameter) of andesitic lava. KfDa is deposited in northeastern and southeastern sides of Kamafusayama. Maximum thickness is 7.0 m at the northeastern side of Kamafusayama.
3. Petrographic characteristics and discussion
Common phenocryst minerals of Ksv, Kav, KfDa and Osd are Pl, Opx, Cpx, Opq. Some samples of KfPD, Ksv and Osd include Qtz phenocryst. Ksv and Osd are low-K dacite to andesite (SiO2=55.6-64.8wt%, K2O=0.21-0.97wt%, and SiO2=60.7-66.2wt%, K2O=0.08-0.97wt%, respectively). Kav shows low-K andesitic compositions (57.4-57.6wt% in SiO2, 0.42-0.43wt% in K2O). SiO2 and K2O contents of lava fragments of KfDa are 59.8-63.7wt% and 0.75-1.15wt%, respectively, categorized in low-K~medium-K dacite to andesite. On plots of Harker diagrams in major elements, Ksv forms similar trends to Eruption stage 1 products of KfPD. Compositional field of lavas in KfDa overlaps with those of Eruption stage1 and 2 of KfPD.
As a result, the source of KfPD can be estimated to be the Kashiasahidake Volcano owing to its distribution, lateral thickness change of air fall units and petrological similarity. We could not identify the source edifice of KfDa because there is no amphitheater on the adjacent volcanoes and petrographic

characteristics of them (Ksv, Kav, Osd) are not similar to lava fragments of KfDa.

5. Reference

1)Yamamoto,T.(1999), 2) Yamoto,T.(2006), 3)NEDO (1990), 4)Takashima.I.,Kumaki.M.(2012)
5)Suzuki.T.,Murata.M.(2008), 6)Murata.M.,Suzuki.T.(2011), 7)Ban.M.,Talapka.N.(1995)

Keywords: Kamafusayama pyroclastic deposits, Kamafusayama debris avalanche deposit, Kashiasahidake Volcano

Paleostress analysis of dike swarms of the V2 arc magmatism in the Oman Ophiolite

*Susumu Umino[1], Yuki Kusano[2], Atsushi Yamaji[3]

1. Department of Earth Sciences, Kanazawa University, 2. Geological Survey of Japan, AIST, 3. Division of Earth and Planetary Sciences, Kyoto University

The world largest and best preserved Oman Ophiolite provides the entire geological records of intra-oceanic subduction zone formation and arc evolution. The fast-spread oceanic crust consisting of 98-96 Ma MORB-like basalt (V1) was followed by 96-94 Ma arc volcanism (V2) on a shallow dipping subduction zone, most likely resulted from microplate rotation including the spreading axis [1-9]. The V2 volcanism was dominated by arc tholeiitic rocks and terminated with sporadic activities of low-silica boninite. Through the V2 magmatism, the same source mantle shows progressive depletion by stepwise melt extraction, as shown by the lower Nb/Ta ratios for the younger volcanic rocks (V2 boninite < V2 tholeiite < V1)[7]. The V2 arc tholeiitic and boninitic magmas were successfully modelled as the results of progressive remelting of the V1 residual mantle promoted by the high-T hydrous fluid and sedimentary melt liberated from the metamorphic sole as evidenced by the eHf(t) and Sr-Nd isotopic ratios of the amphibolite and metachert in the sole and clinopyroxene separates from boninites [8,10].

Although volcanic stratigraphy and geochemical evolution of the V2 arc magmatism are well constrained, the V2 magma plumbing system is poorly understood. The lower V2 tholeiitic strata are widely distributed over 200 km, however, the upper boninitic rocks show only limited and sporadic distribution with the largest exposure in the north between wadis Hatta and Ahin, where boninitic and tholeiitic volcanic rocks are intimately associated with hypabyssal and plutonic equivalents, such as dikes, gabbronorite and gabbros. In the north of Wadi Fizh, intense E-W-striking dike swarms that cross cut the N-S-striking V1-stage sheeted dikes are considered to be the feeders of the V2 flows and pyroclastic rocks and have emanated from diorite-gabbro-gabbronorite-ultramafic cumulate complex, which intruded into and replaced the V1-stage layered gabbros, sheeted dikes and lavas. On the other hand, the V2 feeders in the south of Wadi Fizh are N-S to NW-SE dikes and low-angle sheets, the latter of which locally form intense swarms and were hence interpreted as cone sheets [12]. We investigated the distribution, structure and lithology of the E-W-striking dike swarms to understand the paleostress field and genetic relationships between the dike swarms and the V2 extrusive rocks and the plutonic equivalents. The dike swarms strike mostly in two directions of WNW-ESE and E-W, and forms four dense clusters of dikes 3-4 km in width and every 5 km apart N-S. The most intense swarms consist of 100 % sheeted dikes that appear between the lower plutonic bodies and the upper V2 strata. The paleostress analysis [12] of the E-W dike swarms shows that each swarm of dikes is divided into a couple of group of dikes with different paleostress orientations. All these dikes indicate vertical to steeply dipping maximum compressive stress axis and high magmatic pressure exceeding the minimum compressive stress, indicating intrusions along extensional shear fractures oblique to the minimum stress axis, as shown by the coexistence of dikes with two different orientation.

[1] Umino et al. 1990. Malpas et al. (eds.), Ophiolites, Oceanic Crustal Analogues, 375 - 384 [2] Umino et al. 2003. Geochem. Geophys. Geosyst., 8618 [3] Weiler 2000. Marine Geophysical Res., 21, 195 - 210 [4] Ishikawa et al. 2002. Geology, 30, 899-902 [5] Miyashita et al. 2003. Geophys. Geosyst., 8617 [6] Kusano et al. 2012. Geochem. Geophys. Geosyst., 1, 32 –33 [7] Kusano et al. 2014. Geol. Soc. London Spec. Pub., 392, 177-193 [8] Kusano et al. 2017. Chemical Geol., 449, 206 –225 [9] Tsuchiya et al. 2012. Lithos,

156-159, 120 –138 [10] Umino et al. 2016. Japan Earth Planet. Sci. Joint MeetingSIT09-11 [11] Lippard et al. 1986. Geol. Soc. London Memoir, 11 , Blackwell Sci. Pub. [12] Yamaji 2016. Island Arc, 25, 72 - 1157

Keywords: Oman Ophiolite, V2 arc magmatism, dike swarm, paleostress analysis, boninite, subduction initiation

The magmatic processes of the latest eruption of Hakusan Volcano

*Yuzuki Ibaraki[1], Susumu Umino[1]

1. Kanazawa University

Low-frequency earthquakes were observed for the first time in 1999 at 37 km in depth beneath Hakusan Volcano, which has 400 year-long cyclic activities for the last 1300 years. It is very likely that Hakusan Volcano may have started the next active period. It is critical to understand the current status of the magma reservoirs beneath Hakusan Volcano in order to anticipate the possible styles of the forthcoming eruptions. For this purpose, I studied the latest volcanic products in 17th century of Hakusan Volcano to understand the magmatic conditions.

Hakusan Volcano consists of 4 stratovolcanoes. The latest, Younger Hakusan Volcano began its activity at ca 50 ka. A projectile in the south of the summit craters of the latest eruptions was chosen for detailed analysis of the magmatic conditions.

Together with the disequilibirum phenocryst assemblage, phenocrystic hornblende is decomposed and surrounded by clinopyroxene, orthopyroxene. Rims of orthopyroxene phenocrysts show a wide range, while cores show bimodal compositions. The wide and disequilibrium mineral chemistry and textures, combined with incompatible phenocryst assemblage, led us to conclude the mixing origin for the sample with three magmas: basalt magma, andesite magma, and dacite magma. The plagioclase-hornblende thermobarometry (Holland and Blundy, 1994) was applied to a zoned hornblende with plag inclusions showed the increase in T from 800℃ to 950℃ without changing P, and then gradual increase in both T and P to 1000℃ and 0.9 kb. The final T recorded by the groundmass cpx-opx pairs indicates 1250℃.

The above T-P path suggests that the dacite magma was initially highly crystalline near the solidus at 800℃ and 7-8 km in depth. The dacite magma was injected by the andesite magma that remelted and remobilized the dacite, both of which were partially mixed together and started to ascend. At a depth of ~2.5 km, the basalt magma was injected into the ascended dacite magma batch and triggered the eruption.

Keywords: Hakusan Volcano, magmatic processes, magma mixing, reverse zoning, geothermometer

Eruption history and magma plumbing system of Akanfuji in the Me-akan volcano, eastern Hokkaido, Japan

*Eiichi Sato[1], Keiji Wada[2]

1. Institute for Promotion of Higher Education, Kobe University, 2. Earth Science Laboratory, Hokkaido University of Education at Asahikawa

Akanfuji, situated in the Me-akan volcano of Eastern Hokkaido, started its eruption ca. 2.1 ka, and its activity continued for 1,100 years. During this period, 17 eruption deposits (Akf-1-Akf-17) can be discerned. The mode of the eruptions of this volcano was mainly of the scoriaceous sub-plinian type. Lava flows are often associated with the scoria eruption. The eruption history of Akanfuji is divided into five stages. In the first stage (Akf-1), scoria fall with many lithic fragments was deposited from northeast to east of the volcano. In the second stage (Akf-2-Akf-3), two larger eruptions occurred and coarse scoria falls were deposited to the northeast. In the third stage (Akf-4-Akf-13), some eruptions occurred and the scoria falls were dispersed in a northeast to southeast direction. This stage is characterized by the finding of orthopyroxene in the deposits. In the forth stage (Akf-14-Akf-16), three larger eruptions occurred and voluminous scoriae were deposited to northeast (Akf-14) and from southeast to south (Akf-15-Akf-16). In the final stage (Akf-17), fine scoria fall was deposited from northeast to southeast. Akanfuji had erupted basalts through its history. Two types of basalts (types I and II) are recognized on the basis of phenocrysts assemblage. Type I is orthopyroxene (opx) bearing olivine (ol)-crynopyroxene (cpx) basalt and Type II is cpx bearing ol-opx basalt. Both types show mineralogical evidences of magma mixing, which are reaction products such as cpx overgrowth around opx phenocrysts, wide range of core compositions, and coexistence of normaly and reversely zoned plagioclase, olivine, and pyroxenes. Zoning profiles of these phenocrysts show timing of magma mixing. We can estimate the time from mixing of the basaltic magmas to the eruption.

Keywords: Me-akan volcano, Akanfuji, Magma mixing

Progress of magma mixing by analysis of heterogeneous fragments from Rawan pyroclastic flow at 9 ka, Me-akan volcano, eastern Hokkaido

*Yuma Endo[1], Keiji Wada[1], Eiichi Sato[2]

1. Earth Science Laboratory, Hokkaido University of Education at Asahikawa, 2. Institute for Promotion of Higher Education, Kobe University

At Me-akan volcano, eastern Hokkaido, pyroclastic activity of plinian fall and pyroclastic flows including pumice and scoria have occurred at 13000-12000 years ago, forming Nakamachineshiri crater with 1.1 km diameter (Wada, 1989). At about 9000 years ago, pyroclastic flow containing pumice, scoria and heterogeneous juvenile ejecta such as banded pumice was flowed down along the Rawan river southwestern of Nakamachineshiri crater. We call this Rawan pyroclastic flow. We analyzed the chemical composition of groundmass glass and plagioclase phenocrysts and groundmass in two specimens of each pumice, scoria and banded pumice in detail.
The groundmass composition of scoria shows SiO_2=61-70wt.% and has fixed chemical trend, whereas that of pumice concentrates to SiO_2=77-79wt.%. The scoria part in the banded pumice varies from SiO_2 =61-76wt.% and shows wide compositional range connecting with scoria and pumice compositions. The pumice part in the banded pumice is slightly higher SiO_2 composition (78-80wt.%) than pumice fragment. Plagioclase phenocryst of scoria and pumice shows almost the same bimodal An content distribution of An58-60 peak and An72-92 wide peak. The lower An plagioclase phenocrysts of both scoria and pumice show the same texture, but the high An plagioclase phenocrysts are different origin between scoria and pumice; rapid crystrallization from mafic magma for scoria and long storage in magma chamber for pumice.
These results suggest that each magma produced scoria or pumice was already mixed in the single or plural magma chamber, and mafic magma produced scoria was injected into felsic magma produced pumice to mingle and mix in the conduit. Diffusion rate of mafic magma is faster than that of felsic magma, mixing proceeds inside of mafic magma incorporating felsic magma in central part in the conduit, producing the banded pumice.

Keywords: Me-akan volcano, magma mixing, banded pumice

Petrology of Takikawa monogenetic volcano group and Shokanbetsu volcano: Temporal and spatial variation of magma at the arc-arc junction

*Ryunosuke Enoeda[1], Mitsuhiro Nakagawa[1]

1. Hokkaido University

Takikawa volcanic field is located at the junction of the Kuril and the northeastern (NE) Japan arc. It consists of Takikawa Monogenetic Volcano group (TMV) and some polygenetic volcanoes: Shokanbetsu volcano group (SHV) and Irumukeppu volcano (IKV). These volcanoes were active during late Miocene to early Pleistocene, and have ceased their activity since 1.7 Ma (Nakagawa et al., 1993). TMV exists in the central area of Takikawa volcanic field, composed of basaltic lava cone, dyke and sill. SHV consists of some polygenetic volcanoes with basaltic-andesitic lava flows in the western area of Takikawa volcanic field. IKV, located in the eastern area of Takikawa volcanic field, is a polygenetic volcano, consisting of andesitic lava flow. There are several previous studies about volcanic rocks in this district (Oba, 1972; Yagi et al., 1987; Nakagawa et al., 1993; Okamura et al., 2000). Although several major and trace elements about TMV and SHV are reported, the comprehensive petrological and geochemical features of the volcanic rocks from Takikawa volcanic field have not been still revealed.
Monogenetic volcanoes at this district could have been formed under extensional stress field accompanied with spreading of Takikawa structural basin (Nakagawa et al.,1993). Therefore, the geochemical features of Takikawa volcanic rocks are expected to reflect temporal and spatial variations of magmatism around the junction of the Kuril and the NE Japan arcs during late Miocene to early Pleistocene. These features can provide us the important constraint for understanding the tectonics at the arc-arc junction. In order to reveal the magmatic process at arc-arc junction, we have been carried out the petrological and geochemical study about Takikawa volcanic field. We investigated 17 rock bodies in TMV, three volcanoes of SHV: Minamishokan, Etai and Ofuyu. In this presentation, we report the petrographical features, and major and trace elements of whole-rock chemistry of these volcanic rocks.
Most of rocks in TMV are augite-olivine basalt. They are absent from plagioclase.. Andesite including plagioclase, hypersthene, and resorbed quartz are rarely occurred. In Minamishokan, the rocks in upper part are hypersthenes-augite andesite with plagioclase and mafic inclusion. In contrast, the lower rocks are quartz-bearing olivine basalt, including plagioclase with dusty zone and resorbed quartz with augite reaction rim. The rocks of Etai are clinopyroxene-olivine basalt, having plagioclase with dusty zone and inclusions with glomeroporphyritic texture. Ofuyu is composed of quartz-bearing augite-olivine basalt, similar to those of Etai, except for the existence of resorbed quartz.
Focusing on incompatible elements of the primitive basalt, SHV has relatively narrow range showing relatively higher Rb/Zr and Ba/Zr ratios, and lower Nb/Zr ratio. In contrast, TMV shows relatively wide range with lower Rb/Zr and Ba/Zr ratios, higher Nb/Zr ratio. The various ratios of incompatible elements of primitive basalts in this district cannot be produced by crystallization of a single primary magma, but be derived from multiple various primary magmas. Considering the difference in ratios of incompatible elements primitive basalts, SHV has the feature of island arc basalt (low-Nb/Zr and high-Ba/Zr ratios). TMV exhibits the feature of back arc basin basalt with.high-Nb/Zr and low-Ba/Zr ratios. These spatial distribution of ratios of incompatible elements shows ellipse zonation, similar to the zonation of SiO_2 wt.% reported by Nakagawa et al. (1993). This feature might reflect the difference in degree of partial melting at producing primary magma or the compositional variation in mantle source, corresponding to the mantle plume model under this district, of which SHV as a center, proposed by Nakagawa et al. (1993). In

order to examine this possibility, we are going to carry out the additional geochemical study using rare earth elements and isotopic compositions.

Keywords: Monogenetic volcano group, Shokanbetsu volcano, Arc-arc junction, Basalt, Mantle plume

Formation history and active age of Iwaonupuri Volcano of Niseko volcanic group,southwestern Hokkaido,Japan

*Ryoko Matsuo[1], Mitsuhiro Nakagawa[1]

1. Hokkaido University

Niseko volcanic group (NVG), located at the northern part of southwestern Hokkaido, is Quaternary volcanoes composed of stratovolcanoes and lava domes. There are some previous geological studies about NVG (Hirokawa and Murayama, 1955; Oba, 1960; NEDO, 1986, 1987). It is revealed that NVG started its activity at 1.6 Ma and the active area had moved from west to east. It is believed that Iwaonupuri volcano is the youngest volcano in NVG on the basis of the fresh morphology as well as fumarolic activity. Okuno (2003) reported the ^{14}C age from the soil beneath Iwaonupruri tephra: ca.6 ka. However, he also indicated the low reliability of this ^{14}C age, and the source and eruption style of this tephra are still unclear. Therefore, in order to reveal the eruptive history and eruption style of the NVG, especially in Holocene epoch, we performed geological study about NVG.
Iwaonupuri and Nitonupuri have been considered as the youngest volcanoes in NVG. The rocks of both volcanoes are andesite, containing plagioclase, clinopyroxene, orthopyroxene, and magnetite phenocrysts. In addition, the rocks of Nitonupuri have hornblende. On whole-rock chemistry, Iwaonupuri can be clearly distinguished from Nitonupuri on many Harker diagram. According to vent location, stratigraphical relationships, petrological features, it is considered that these two volcanoes are the distinct ones. Therefore, we define the volcano has been active after the activity of Nitonupuri as Iwaonupuri, which is the youngest one in NVG.
Iwaonupuri (1,116 m a.s.l.) is located at the eastern part of NVG. This volcano has been built on the east of Nitonupuri, composed of a pyroclastic cone and several lava domes and lava flows. Iwaonupuri Big Crater pyroclastic cone (IBC) with a crater (ca. 1km in diameter) locates at the western part of Iwaonupuri. Sho-Iwaonupuri lava dome (SI) exists in this crater. IBC and SI are covered with the Dai-Iwaonupuri volcanic edifice (DI). DI consists of the lower lava dome and the upper lava flows distributed from the summit to the east. In addition, several small craters such as Gosikionsen crater are found in the whole area of Iwaonupuri. Iwaonupuri volcano can be divided into five units on the basis of stratigraphic relationship, eruption style and the location of the eruptive center: IBC pyroclastic rocks, SI lava dome, DI lower lava dome, DI upper lava flows, and Iwaonuouri phreatic explosion breccia in ascending order.
The activity of Iwaonupuri started with forming IBC. At first, phreatic eruptions occurred. After that, its activity changed to the magmatic eruptions, forming eruption column and generation pyroclastic flows intermittently. This activity provided NsIw-1 tephra found by Okuno (2003). The thickness as well as the grain size of component in this tephra become larger from east to west, suggesting that this tephra can be correlate with IBC. In this study, we obtained two ^{14}C ages: 9480 cal.yBP from the charcoal in the pyroclastic flow and 10910 cal. yBP from the soil beneath the NsIw-1 tephra. Accordingly, it is concluded that Iwaonupuri started its eruptive activity about 9,500 years ago and has extruded lava domes and lava flows repeatedly. It is also considered that phreatic and phreatomagmatic eruptions were occurred contemporaneously, to form many explosion craters in the whole area. Although the latest magmatic eruption is DI upper lava flows from the summit, the phreatic eruptive activity would have continued after this eruption. Actually, we obtained "Modern" as the result of the ^{14}C age from a layer of explosion breccia near Gosikionsen spa. In this study, we revealed the age of the initial stage of Iwaonupuri eruptive activity. Considering the eruption age at 9,500 years ago, the growth history of volcano and the existence of many young explosion craters, it is probable that Iwaonupuri is the volcano with high level of activity through Holocene epoch.

Keywords: Iwaonupuri, formation history, active volcanoes, geology, radiocarbon dating, Niseko volcanic group

Reexamination of late Pleistocene tephras of Shikotsu-Toya Volcanic Field

*Mizuho Amma-Miyasaka[1], Mitsuhiro Nakagawa[1], Daisuke MIURA[2], Shimpei Uesawa[2], Ryuta FURUKAWA[3], Akiko Matsumoto[1]

1. Hokkaido University, 2. Central Research Institute of Electric Power Industry, 3. Advanced Industrial Science and Technology

Shikotsu-Toya volcanic field (STVF) in southwestern Hokkaido is located at an arc-arc junction of Kuril and NE Japan arcs, and composed of three caldera volcanoes (Shikotsu, Toya and Kuttara) and Yotei & Shiribetsu stratovolcanoes. Advanced tephrochronological studies have been undertaken to establish the sequence of the pyroclastic flow and pyroclastic fall deposits in STVF (Kasugai et al., 1980; Yamagata, 1994; Machida, 1999). Combined with precise AMS ^{14}C dating and Marine Oxygen Isotope Stage (MIS) determinations, explosive eruptions have been repeated during 130-40 ka (Yamagata, 1994; Katoh et al., 1995; Machida and Arai, 2003; Sase et al., 2004). However, stratigraphy of these tephras has not been revised since 1990's and identification of tephra layers was mainly based on petrography and refractive index of glasses for the caldera volcanoes. Furthermore, it is suggested that Yotei and adjacent Shiribetsu volcanoes has erupted since ca. 50 ka (Nakagawa et al., 2011; Uesawa et al., 2016).
In this study, geological survey has been done mainly in southern and eastern part of lake Shikotsu (< 65 km). Pyroclastic flow deposits of Shikotsu caldera-forming eruption widely and thickly covered around the lake, we also carried out boring explorations in the proximal area (10 km and 25 km east from the lake center), and observed two cores of Japan Meteorological Agency (10 km south) and National Research Institute for Earth Science and Disaster Prevention (25 km SSE). We used four thick tephra layers as key beds in STVF; Spfa-1 & Spfl, Kt-1, Ssfa & Ssfl and Toya. To correlate tephra layers, we firstly investigate stratigraphic relationships with key tephra layers and then compare petrological characteristics with proximal samples. Then, we distinguished at least 27 tephra layers in STVF, and discovered six new tephra layers in this study. As a results, the beginning of eruptive activity dates back to 120 ka for Shiribetsu volcano and ca. 80 ka for Yotei and Shikotsu volcanoes.
Together with K-Ar ages of volcanic rocks around this area, eruptive history of STVF are summarized as follows. Andesite volcanism had occurred until middle Pleistocene and had terminated around 0.6-0.5 Ma. After a long dormancy (ca. 400 ky), STVF started its eruptive activity 130 ka at Toya, and 120 ka at Yotei volcanoes. A catastrophic caldera-forming eruption occurred ca. 110 ka at Toya volcano. Then, the activity has propagated toward the east. Kuttara and Shikotsu volcanoes started their activity almost simultaneously ca. 90 and 85 ka, respectively. Subsequently, a large stratovolcano; Yotei has been also constructed since ca. 75 ka at the back-arc side of the STVF. The explosive eruptions of VEI=5-6 had repeated at Kuttara and Shikotsu volcanoes, and VEI=6 eruption occurred at Kuttara, and the largest caldera-forming eruption in the STVF occurred at Shikotsu volcano (VEI=7) ca. 45 ka. Since then, Yotei and post-caldera volcanoes in STVF have continued their eruptive activity until now. It should be noted that there exist three active periods during 130-110 ka, 95-75 ka and 60-45 ka in STVF.

Keywords: tephras, late Pleistocene, Shikotsu-Toya Volcanic Field, glass composition

Eruption history of pre-Goshikidake, Zao volcano

*Yuki Nishi[1], Masao Ban[2], Oikawa Teruki[3]

1. Graduate School of Science and Technology, Yamagata University, 2. Department of Earth and Enviromental Science, Faculty of Science, 3. Advanced Industrial Science and Technology

Introduction
Zao volcano is an active stratovolcano in NE Japan, and has a long-eruption history of ca. 1 million years. At the beginning of the newest stage (ca. 35 ka to present), horseshoe shaped Umanose caldera was formed in the summit area. The Goshikidake, the youngest cone, has grown up in the caldera from ca. 2 ka and now its relative elevation are about 110m and bottom diameter is about 850m. The present crater lake Okama is in the western part of the Goshikidake and its diameter about 360 m. The Okama has been active since ca. 0.8 ka and the pre-crater was southeast ward of the Okama. Former studies showed that the cycles from phrenetic to phreatomagmatic eruptions repeatedly occurred, delimited by dormant time. We examined the eruption history during ca. 2 to 0.8 ka based on near vent facies features.
Pre Okama-Goshikidake
Previous study subdivided Goshikidake pyroclastic rocks into 5 units by angular unconformities. Unit 1, 2, 3 were formed during ca 2 ~ 0.8 ka. We define an edifice composed of unit 1~3 products as the pre-Goshikidake. The unit 1~3 products are well exposed in the southern part of the Goshikidake. Our study is based on observation of the products exposed in this area.
unit1
The maximum total thickness of unit 1 is about 20 m. Based on the lithofacies, we subdivided unit 1 products into 7 layers. Layer 1 and 2 are composed of lapilli-tuff. The matrix is hydrothermally altered clay. Layer 1 and 2 are different in color. Layer 3, 5, 7 are composed of strongly stratified thin layers of tuff to lapilli-tuff, showing various kinds of lamination and sagging. Matrix color is gray in layer 3, and raddish brown layer 5 and 7. Layer 4 and 6 are composed of tuff-breccia, including reddish ~ gray colored scoria.
unit2
The maximum total thickness of unit 2 is about 20 m. These products are subdivided into 4 layers. Layer 1, 4 are composed of strongly stratified thin layers of tuff to lapilli-tuff, showing various kinds of lamination and sagging. The matrix is gray to red-radish ash and scoriaceous bombs and volvcanic blocks concenrated parts are sometimes observed. Layer 2 is composed of agglomerate with various amounts of volcanic bombs and scoria. Layer 3 is composed of strongly laminated tuff, its lower is gray and upper is red in color.
unit3
The maximum total thickness of unit 3 is about 20 m. These products are subdivided into 7 layers. Layer 1, 3, 5 are composed of gray colored tuff, and change in quality with small scoria little bit. Layer 2, 4 are composed of strongly stratified thin layers of tuff to lapilli-tuff, showing various kinds of lamination and sagging. The matrix is radish~red-radish ash and scoriaceous bombs and volvcanic blocks concenrated parts are sometimes observed. Layer 7 include both facies. Layer 6 is scoria fall deposit with ~2 m scoria in the scoriaceous matrix. This is observed in southeast and gets thin rapidly to southwest.
The eruption sequence of pre-Goshikidake
Based on these observations, layer 1, 2, 3 of unit 1, layer 3 of unit 2, layer 1, 3, 5 of unit 3 would be by phrenetic eruption products, while layer 4, 5, 6, 7 of unit 1, layer 1, 4 of unit 2, layer 2, 4 of unit 3 would be formed by the phreatomagmatic eruption. Layer 7 of unit 3 include both types. The layer 2 of unit 2 would be vulcanian type like eruption, layer 6 of unit 3 would be scoria fall products.
In the unit 1, the activity began by phrenetic eruptions and changed to phreatomagmatic eruptions. The

unit 2 activity is characterized by repeat of phreatomagmatic eruptions. In the middle part, vulcanian type like and phrenetic eruptions would occur. In the unit 3, the cycle of phrenetic to phreatomagmatic eruptions repeated several times. The strombolian type eruption additionally occurred in the climax.

The migration of the crater location

The crater of unit 1 would be located slightly eastward of pre-crater, based on strike and dip data of unit 1 products. The unit 2 and 3 products were erupted from the pre-crater, revealed by tracking the unit 2 and 3 layers to the eruption center ward. Considering the present crater is in west ward of the pre-crater, the crater migrated stepwise from east to west past ca. 2 ky.

Keywords: Zao volcano, Goshikidake, Eruption history, Pyroclastic surge

Glaciovolcanic and magmatic evolution of Ruapehu volcano, New Zealand

*Chris Conway[1], Colin Wilson[2], John Gamble[2], Graham Leonard[3], Dougal Townsend[3]

1. National Museum of Nature and Science, 2. Victoria University of Wellington, 3. GNS Science

Chronostratigraphic studies of continental arc stratovolcanoes reveal the timing and types of past eruptive behaviour and are therefore crucial for constraining magma evolution models as well as the future eruption potential in these active settings. Such studies can be complicated by complex stratigraphic relationships caused by glaciovolcanism (eruptions in the presence of ice), glacial erosion and sector collapse for edifices that have been glaciated. These issues are relevant to the numerous high-altitude cones that define Earth’ s continental volcanic arcs. A key example of this is Ruapehu, which is an active andesite-dacite stratovolcano located at the southern end of the Taupo Volcanic Zone, New Zealand. The growth of the Ruapehu edifice has occurred throughout coeval eruptive and glacial histories since ~200 ka. Here, new high-precision $^{40}Ar/^{39}Ar$ ages and whole-rock major and trace element data for Ruapehu lava flows are integrated with geological mapping and glacier reconstructions. The data provide a high-resolution chronostratigraphic and geochemical framework for investigating processes of ice-marginal lava flow emplacement and magma generation. In particular, the following concepts are addressed in this study: (1) the potential for ice-bounded lava flows to provide paleoclimate information; (2) the role of deglaciation in triggering Holocene sector collapses; (3) the variable extent of crustal assimilation in andesite-dacite magma genesis during the lifetime of a stratovolcano.

Keywords: lava-ice interaction, andesite petrogenesis, Ruapehu volcano

Formation process of plagioclase aggregates of the 1991-1995 eruption at Unzen

*Yuriko Konishi[1], Atsushi Toramaru[2]

1. Department of Earth and Planetary Science, Graduate School of Science, Kyushu University, 2. Department of Earth and Planetary Sciences, Faculty of Sciences, Kyushu University

We conduct the petrographical description, the textual analysis including crystal size distribution (CSD) analyses and chemical analyses for plagioclase phenocrysts which show frequently the aggregate texture in volcanic rocks of the eruption. In this study, to know the basic information before discussing the magmatic system of the 1991-1995 eruption at Unzen, we focus on plagioclase aggregates and their formation process. Plagioclase phenocrysts can be classified into two types on the basis of textural observation using optical microscopes. Type S phenocrysts exist as a Solo crystal without forming aggregates. Type A phenocrysts have the Aggregate texture in which a phenocryst recognized in hand specimen consists of two to several single crystals. The dusty zone can be found in both types. We conduct CSD analyses for type S, type A and component crystals of type A (type A_{comp}). We conduct chemical analyses for cores and rims of type S and type A_{comp}. Results from CSD analyses show that CSD plots of all types follow the exponential distributions. It is remarkable that CSD plots of type S have steeper slopes and smaller maximum crystal sizes than those of type A_{comp} have. Results from chemical analyses also show the difference in core Anorthite (An) contents; type S has broader range (around An 35-60) than type A_{comp} has (around An 40-55). These results suggest the difference in a magmatic system where each type of plagioclase phenocrysts has crystallized. We propose two models that can explain the characteristics of CSD plots and core An content of the plagioclase phenocrysts; the coalescence model and the separation model. Assuming the coalescence model, we suggest that nucleation rate has increased at a certain time and aggregations have occurred at a certain time interval. On the other hand, assuming the separation model, we suggest that the injection of a high-temperature mafic magma including high-An solo crystals has melted country rocks including plagioclase with core An 40-55. We also suggest that fragments separated from country rocks have assimilated with the mafic magma. Because the slight differences in the CSD trends and the compositional ranges between type S and A_{comp}, which has been detected in this preliminary analysis, may be an important clue to discriminate which process is realistic, we will have to conduct more comprehensive and detail analysis including correlations between size and compositions, trace element compositions, etc.

Keywords: Crystal size distribution, Plagioclase, Aggregate, Mt. Unzen

Modeling the chemical evolution of open-system magma chambers using the principles of heat and mass transfer and thermodynamics

*Koshi Nishimura[1]

1. Toyo Univ.

A model of the chemical evolution of open-system magma chambers has been developed using the principles of heat and mass transfer, and thermodynamics. Generally speaking, thermal Rayleigh numbers for high-temperature, crystal-poor magma chambers are very large, resulting in vigorous thermal convection (Martin et al., 1987). However, convection is suppressed following ~50% crystallization because of the formation of an interlocking framework of crystals. This study focuses on the earlier convection stage of sheet-like magma chambers, prior to significant crystallization.
The model incorporates the effects of concurrent magma influx (recharge or mixing), roof-rock assimilation, magma extraction, and fractional crystallization. Magma influx affects magma composition and temperature, while the rate of roof-rock assimilation is controlled by convective heat flux from the magma and the effective fusion temperature of the roof rock (Huppert and Sparks, 1988; Koyaguchi and Kaneko, 1999). Crystal settling occurs at the floor of the magma chamber (Martin and Nokes, 1988). Equilibrium phase relations and the partitioning of major elements between mineral phases and coexisting liquid are calculated thermodynamically using the rhyolite-MELTS algorithm (Gualda et al., 2012). Trace element and isotopic variations of the magma are calculated using open-system chemical mass balance equations (Nishimura, 2012).
The model quantifies the evolution paths of major and trace elements, and isotopes within crystals, liquid, magma, and crystal rims. Of note, it also shows that the rate of magma influx strongly affects crystal core-to-rim profiles of trace-element concentrations and isotopic ratios.

Keywords: magma chamber, geochemical model, heat and mass transfer

Magmatic plumbing system of a complex ocean island volcano, Ascension Island, south Atlantic

*Katy Jane Chamberlain[1], Katie Preece[2], Jenni Barclay[3], Jane H Scarrow[3,4], Richard J Brown[5], Jon P Davidson[5], Darren Mark[2]

1. Japan Agency for Marine-Earth Science and Technology, 2. SUERC, East Kilbride, UK, 3. University of East Anglia, Norwich, UK, 4. University of Granada, Granada, Spain, 5. Durham University, Durham, UK

Ascension Island, 7°56’S, is an isolated composite volcano in the south Atlantic, lying 90km west of the Mid Atlantic Ridge. Even though Ascension Island is small –only 12 km in subaerial diameter –it has produced a wide variety of eruptive products in its 1-million-year subaerial eruptive history. Volcanic rock compositions range from basalt to rhyolite, following a silica-undersaturated subalkaline evolutionary trend. Yet, while a huge variation in magmatic compositions have been erupted across a limited spatial extent, there is little evidence for magma mixing preserved in erupted deposits.

Here we present extensive whole rock XRF data coupled with EPMA and LA-ICPMS analyses of glass and crystals of samples which span the entire range in compositions erupted throughout Ascension Island’s subaerial history. These new geochemical data are coupled with detailed field observations and targeted $^{40}Ar/^{39}Ar$ dating, which reveal more than 70 explosive pumice-producing eruptions, and more than 40 mafic effusive eruptions have occurred in the last 1-million years. We use these data to construct a robust volcanic history for Ascension Island, including dating its most recent activity, and build a detailed petrological model for the magmatic plumbing system underlying Ascension. These data highlight the role of fractional crystallisation in the production of the range of magmatic compositions found on Ascension Island, and reveals the closed-system nature of the magmatic plumbing system, unlike many other ocean islands, such as Tenerife or Iceland. SIMS-measurements of volatiles in melt inclusions in two zoned fall deposits appear to show this closed-system evolution occurs at depths between 7 and 11 km, i.e. the lower crust. The closed-system and relatively deep nature of magmatic evolution, and the relatively small volumes erupted in single events means that any explosive future activity is unlikely to preceded by significant precursory signals.

Keywords: Ocean Island Volcanism, Magmatic evolution, Crustal Structure

Raman spectroscopy applied to reveal the oxidation state of the “Red” obsidian from Shirataki, Hokkaido, Japan

*Kyohei Sano[1], Eiichi Sato[2], Keiji Wada[3]

1. Shirataki-Geopark, 2. Kobe University Institute for Promotion of Higher Education, 3. Hokkaido University of Education at Asahikawa

Silicic volcanism ranges from explosive to effusive. Understanding what controls in such activity is an important issue to explain the explosive-effusive transition. The recent observation on Cordon Caulle (Chile, 2011–12) revealed that explosive-effusive hybrid activity (Schipper et al., 2013) and the oxidation state in volcanic products have attracted attention to reveal the effusive-explosive transition during magma ascent, especially on viscous magma eruptions (e.g. Castro et al., 2014). The Laser Raman spectroscopy is expected to give information about micro-scale oxidation state based on the specification of oxide microlite and glass amorphous structure in volcanic rocks.
At the Akaishiyama obsidian lava on Shirataki, northern Hokkaido, Japan, we can observe the red-colored oxidized obsidian mingled with black-colored obsidian. The mingled shows various contrasts and distributions on the hand specimen, and we can consider that such a various oxidation texture reflect the different mechanisms of outgassing process during the eruption. In this study, we used the microRaman spectroscopy to characterize the oxidation state in the obsidian, using a JASCO NRS-7100 Laser Raman Spectrometer with 514 nm excitation at Kobe University Research Facility Center for Science and Technology, Japan. We obtained the 2 types of Raman spectra of oxide microlites in red and black obsidians, respectively. Compared with referential spectra, we identified captured spectrum as magnetite and hematite. Based on the analytical results of microRaman Spectrometer and distribution pattern of oxidation texture, we can discuss the formation process of heterogeneous oxidation textures during the eruption.

Keywords: obsidian, Raman spectroscopy, textural analysis, Shirataki

Petrographic description and density analysis of fall deposit by the May 18, 1980, eruption of Mount St. Helens.

*Haruka Ino[1], Atsushi Toramaru[2]

1. Department of Earth and Planetary Sciences, Graduate School of Sciences, Kyushu University, 2. Department of Earth and Planetary Sciences, Faculty of Sciences, Kyushu University

The May 18, 1980, eruption of Mount St. Helens, Washington, erupted white pumices that have the same composition from 08:32 to 18:15 LT. Characteristics of eruption of Mount St. Helens are represented by the dramatic land slide and subsequent plinian eruptions. Phenocrysts and pheno-bubble textures of fall deposits record state in the conduit just before the plinian eruptions. In this study, correlations between texture of fall deposit and time evolution of eruption are examined. Samples of this study were taken from fall deposits divided into seven layers with 2 cm in thickness. The uppermost layer is referred to as layer 1, layers below are identified by following sequential integers. Measurement of bulk density and description of texture were carried out for white pumices with 8~16mm in radius in each layer. Bulk density was calculated on the basis of bulk volume by 3D image. Thin sections were made for white pumices with the average in mass, bulk volume and bulk density in each layer and the maximum and minimum bulk density in layer 1. Measured bulk density ranges 0.495~1.01g/cm³. Statistical made of bulk density is 0.7~0.8g/cm³in the intermediate bin for layer 1 and 2, whereas that is in the smallest bin 0.5~0.6g/cm³ and the abundance of pumices monotonically decrease with bulk density for layer 3 and 4. Layers 1 and 2, as well as layers 3 and 4 resemble in bulk density distribution and petrographic texture. Specifically in the petrographic texture, there are more phenol-bubbles for layer 3 and 4. The maximum and minimum bulk densities **in layer 3** are 0.888g/cm³ and 0.505g/cm³, respectively. From backscattered electron images, pumices samples with minimum density include more coalesced bubble than those with maximum one. If we assume the inverse relationship between eruption intensity and pumice bulk density, we can suggest that pumices with the smallest bulk density in layer 4 may be eruption products when the plinian column grew up to the maximum height. We should confirm the trend in texture of pumices by more detail analysis for sufficient numbers of pumices samples with different bulk densities in each layer including bubble size distribution measurement and chemical analysis microlites. Furthermore, from BSD data we should calculate the average bubble nucleation rate and growth rate to infer how bubbles were formed, in addition to the estimation of buoyancy state of the conduit prior to eruptions by pheno-bubble abundance.

Keywords: vesicularity, plinian eruption, density, pheno-bubble

Textural analysis of Blast deposits from the May 18, 1980, eruption of Mount St. Helens

*Mizuki Takehara[1], Atsushi Toramaru[2]

1. Department of Earth and Planetary Sciences, Graduate School of Sciences, Kyushu University, 2. Department of Earth and Planetary Sciences, Faculty of Sciences, Kyushu University

On 18 May 1980 at 08:32 LT, the northern flank of Mount St. Helens (in southern Washington State, USA) collapsed by an M5 earthquake. The landslide caused a giant lateral "Blast" originating from cryptodome. Hoblitt and Harmon (1993) reported two juvenile rock types - gray dacite and black dacite - that are derived from the same cryptodome magma. They are different in bulk density, but their textures have not been analyzed in details. In the present study, therefore, we carry out the textural analysis of two cryptodome dacite - gray dacite and black dacite -, and discuss processes that may have generated two different types of products.

Samples were taken from five layers of deposits at two sites –STOP 6 and STOP 7-. STOP 7 is 45° clockwise from north about 5 km from the vent. STOP 6 is 70° clockwise from north about 10 km from the vent. Samples from three layers, "upper", "middle", and "lower" were taken at STOP 6. Samples from two layers "upper" and "lower" were taken at STOP 7. We made a following analysis. (1) Grain size analysis, (2) Component analysis (8-16 mm), (3) Bulk density (8-16 mm), (4) Texture analysis (void and crystal). In analysis of grain size distribution, we sieved the five samples by $2^{-\phi}$ mm metal mesh sieve (ϕ = 2, 1, 0, -1,-2, -3 -4 -5). As the result, it is found that the average grain size of STOP 6 is larger than STOP 7. On the basis of color and vesicularity of grains, we classified each 8-16mm samples into four types ("gray dacite", "black dacite" "lithic", and "others"). As the result, it is found that gray dacite and black dacite occupy 70-80 % in volume at each layer. Also, deposit at STOP 7 include more black dacite than at STOP 6. We measured bulk volume of all particles of gray and black dacites with 8-16 mm at each sites by the 3D scanner, and calculated bulk density. As the result, the density of juvenile dacites shows clear bimodal distribution, with peaks at 1.9 gcm^{-3} (gray dacite) and 2.3 gcm^{-3} (black dacite). We observed the texture (void and crystal) of 8-16 mm gray and black dacite particles that represent each layer by reflection microscope and SEM. As the result, although both of them has microlites (small crystals of 1 μ-30 μm) in groundmass, they have quite different textural characteristics as follows: Gray dacites show uniform distribution of rounded vesicles with various sizes (1 μ-200 μm) whereas black dacites show remarkable heterogeneity in vesicle abundance and morphology, that is void-free regions and void-rich regions consisting of angular voids (0.1-1 mm) surrounded by microlites. In addition, in black dacites cracks develop connecting the void-rich regions regardless of presence of phenocryst and groundmass.

From results of the textural study, we speculate that gray dacites had experienced decompression vesiculation, whereas, black dacites had experienced vesiculation by cooling crystallization before the sadden decompression. We suggest that, a first rising magmas corresponding to black dacites had been cooled and crystallization-induced vesiculation at the location close to the surface, and a magmas beneath the cooled magma in cryptodome, corresponding to gray dacites, had preserved relatively large amount of volatile component. Thus, the landslide made cracks in the black dacite magmas by brittle fracturing and bubbles in the gray dacite magmas by vesiculation. Such differences in volatile contents and history in vesiculation and crystallization result in the textural difference revealed by this study.

Keywords: Mount St. Helens, cryptodome, blast

